GEOPHYSICAL RESEARCH LETTERS, VOL. 25, NO. 17, PAGES 3367-3370, SEPTEMBER 1, 1998

Global Variations in Droughts and Wet Spells: 1900-1995

Aiguo Dai and Kevin E. Trenberth

National Center for Atmospheric Research, Boulder, Colorado

Thomas R. Karl

NOAA National Climatic Data Center, Asheville, North Carolina

Abstract. The Palmer Drought Severity Index (PDSI) was calculated globally using gridded monthly air temperature and precipitation. From 1900 to 1995, there are large multi-year to decadal variations in the percentage areas in severe drought (PDSI < -3.0) and severe moisture surplus (PDSI $> +3.0$) over many land areas while secular trends are small. Since the late 1970s, however, there have been some increases in the combined percentage areas in severe drought and severe moisture surplus, resulting from increases in either the drought area (e.g., over the Sahel, eastern Asia and southern Africa) or both the drought and wet areas (e.g., over the U.S. and Europe). Although the high percentages of the dry and wet areas in the recent decades are not unprecedented during this century (except the Sahel), the recent changes are closely relate to the shift in El Niño - Southern Oscillation (ENSO) towards more warm events since the late 1970s and coincide with record high global mean temperatures. Moreover, for any given value of ENSO indices, the PDSI anomalies tend to be larger than would be expected from previous records. These changes are qualitatively consistent with those expected from increased greenhouse gases in the atmosphere.

Introduction

Extreme climate events, such as droughts and floods, by their very nature are rare. Consequently they are located at the tails of distributions of climate variables and percentage-wise will change more rapidly than the mean in a changing climate. Global climate models (GCMs) [*Kattenberg et al.*, 1996; *Gregory et al.*, 1997] indicate that in a warmer climate droughts may become longer lasting and more severe in current drought-prone regions because of enhanced evaporation, and, because of increased atmospheric moisture, precipitation events may become more intense, leading to more flooding. Over the U.S., the climate has become more extreme in recent decades [*Karl et al.*, 1995; *Karl and Knight*, 1998]. In the Sahel, extreme droughts have persisted most of the time during the last 2-3 decades [*Nicholson*, 1993]. Over Australia, for any value of the Southern Oscillation Index (SOI) the rainfall and daily maximum temperature tend to be higher after the 1970s than would be expected for such an SOI in the earlier decades [*Nicholls et al.*, 1996b].

Paper number 98GL52511.
0094-8534/98/98GL-52511$05.00

The 1995 IPCC report [*Nicholls et al.*, 1996a] reviewed the evidence for changes in extreme weather events. Here we examine the variations in meteorological droughts and wet spells over the global land areas during this century using the popular Palmer Drought Severity Index (PDSI) [*Palmer*, 1965], a proxy of soil moisture content. We focus on decadal variations in the percentage areas in severe drought or severe moisture surplus and their association with ENSO, and we find that the change in the relationship between SOI and rainfall found by *Nicholls et al.* (1996b) also exists over other regions.

Data

The PDSI is calculated using monthly air temperature T (*Hansen and Lebedeff*, 1987 and updates) and precipitation P (*Dai et al.*, 1997) based on a moisture balance on the ground. Anthropogenic changes in surface conditions that alter the drainage catchment or runoff are not considered in the index. The PDSI has been widely used in the study of U.S. droughts despite its limitations [*Alley*, 1984]. The PDSI generally ranges from -7.0 (dry) to $+7.0$ (wet) with histograms fairly close to normal distributions. We evaluated the PDSI with available streamflow and soil moisture data and found that the PDSI can capture a large portion of the multi-year to decadal variations in these hydrological variables (cf. Fig. 1). This suggests that the PDSI is a useful proxy of moisture conditions on the ground. We should, however, only expect a qualitative agreement between the PDSI and streamflow data, because the latter indicate hydrologic droughts and floods which depend on not only meteorological conditions, but also other factors such as dams and reservoirs.

There are various errors in the station-record derived T and P datasets (on a 2.5^ox2.5^o grid), especially for precipitation. *Dai et al.* (1997) made adjustments to correct the major inhomogeneity errors in station precipitation records and showed that reliable decadal to long-term changes can be derived from the precipitation dataset. Although not perfect, the spatial and temporal coverage of the T and P datasets are much better than the instrumental records of other climate variables. We used the soil-texture-based water-holding capacity map from *Webb et al.* (1993) and kept it unchanged during the the period (1900-95) of the PDSI calculation. Tests showed that the results are insensitive to the values of water-holding capacity. The calibration base period of the PDSI calculation is from 1950 to 1979.

The streamflow data used in Fig. 1 are from *Slack* (1993) for the U.S., *Simpson et al.* (1993) for S.E. Australia (135^{o}E-

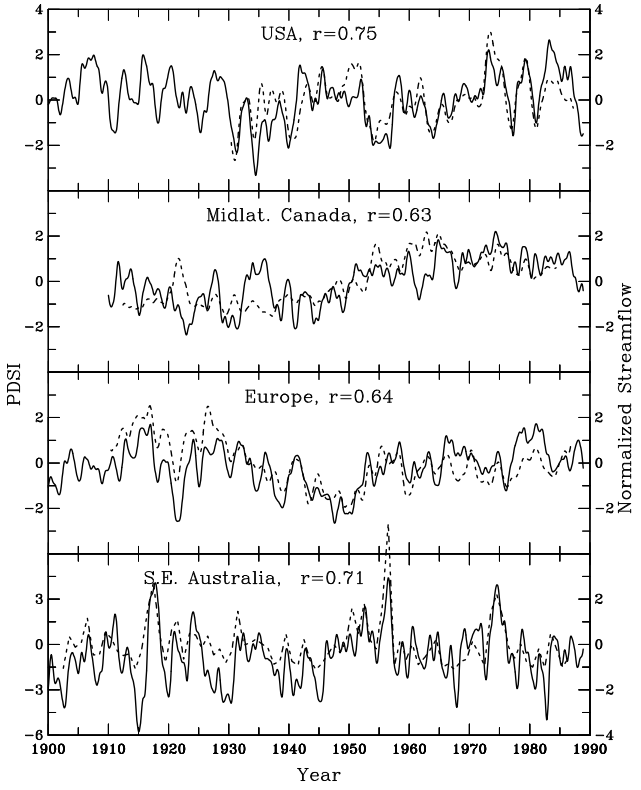

Figure 1. Area-averaged regional PDSI (solid line) and streamflow (broken line). Variations with periods < 24 months in the averaged time series were filtered out. The correlation coefficient r between the two curves is significant at <1% levels for all the regions (the reduction in the number of degrees of freedom by the autocorrelation in the time series was considered in all the tests performed in this study).

153°E, 40°S-33°S) (River Murray and Darling), and *Barnes* (1995) for Europe (west of 50°E) and mid-latitude (south of 60°N) Canada. The U.S. and Australian streamflow data are fairly reliable and have been used in many climate studies. The European and Canadian streamflow data have good temporal and spatial coverage and seem to be reliable. Streamflow data for other regions are insufficient for comparison with the PDSI. We derived the regional averages of streamflow for the U.S., Europe and mid-latitude Canada by averaging the station discharge records using drainage areas as weighting (thus emphasizing the downstream discharges which largely integrate upstream flows).

Results

Fig. 1 compares the area-averaged monthly PDSI with streamflow over the U. S., mid-latitude Canada, Europe and S.E. Australia. Both the PDSI and streamflow have large multi-year and decadal variations and they are significantly correlated on these time scales. Arid regions contribute little to the PDSI−streamflow relationship shown in Fig. 1. For example, the U.S. PDSI−streamflow relationship is strong in the central (correlation coefficient r=0.79 and eastern (r=0.69) U.S. and becomes poor (r=0.10) over the western (west of 115°W) U.S. This is expected because more rainfall evaporates instead of going into streamflow in arid areas such as the western U.S. The widespread drought conditions over the U.S. in the 1930s, middle 1950s and 1988 are evident in both the PDSI and streamflow records. Europe (mostly central Europe) experienced prolonged droughts from the 1940s to early 1950s. In mid-latitude Canada, the latter half of the 20th century is considerably wetter than the earlier decades. Over S.E. Australia, multi-year variations, which are often induced by ENSO events, predominate although decadal changes also exist. The gridded PDSI is also significantly correlated (r=0.45 to 0.73, with $r \geq$0.28 being significant at a 1% level) with soil moisture observations [*Vinnikov and Robock*, 1996] from former U.S.S.R. stations.

Karl et al. (1995) examined the percentage areas in severe droughts and severe moisture surplus over the U.S. Fig. 2 shows the percentage areas together with the sum of the two for the regions where data are sufficient. It can be seen

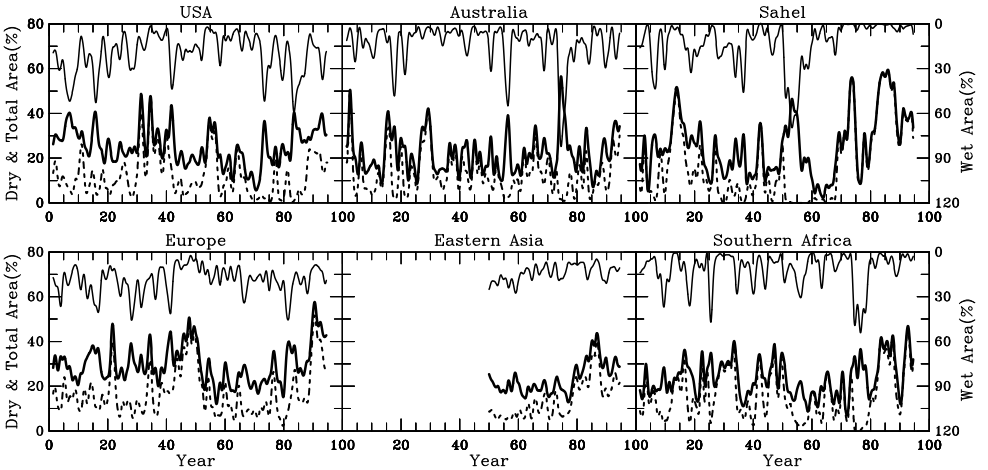

Figure 2. Percentage areas in severe drought (PDSI< −3.0, *dashed lin e*), severe moisture surplus (PDSI> +3.0, *thin solid line*), and the sum of the two (*thick solid line*) over the regions where data are sufficient during the plotted periods. Note that the wet area is plotted using the downward scale on the rightside ordinate (0 to 80% except Sahel and S. Africa) and the dry and total area scales are from 0 to 120% on the leftside ordinate for Sahel and S. Africa. Variations with periods < 24 months were filtered out.

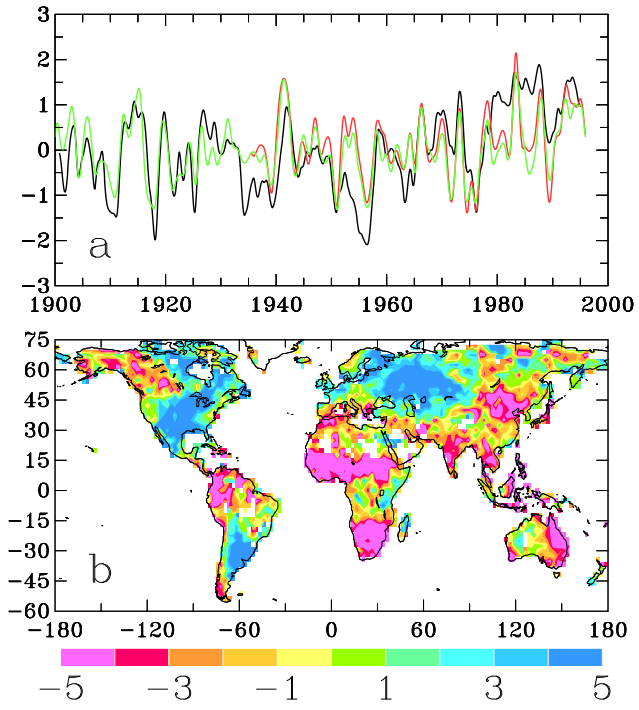

Figure 3. Temporal (*a*, black line) and spatial (*b*) coefficient s of the first leading EOF of the monthly PDSI (normalized by its standard deviations prior to the EOF analysis, the pink and red areas are dry and the blue areas are wet in El Niño years). Also shown in the upper panel are the SOI (red line, sign flipped) and the normalized Darwin sea level pressure index (green line) [*Trenberth and Hoar,* 1996]. Variations with time scales < 24 months are filtered out for both the EOF temporal coefficient and the ENSO indices. The smoothed ENSO indices are shifted to the right by six months in order to obtain the maximum correlation between the EOF coefficients and the ENSO indices (i.e., the ENSO indices lead the EOF coefficients by six months). The correlations (r=0.61 with the SOI and r=0.67 with the Darwin pressure index) are significant at <0.001% levels.

that the multi-year and decadal variations in the percentage areas are very large. For example, over the Sahel on average about 50% of the region has been in severe drought since 1970, which is about twice that in the first half of the century. While the severe dry and wet areas are negatively correlated, the sum of the two still has large variations (Fig. 2). For example, the percentage area over Europe in relatively normal conditions was ∼60% in the 1940s and increased to ∼80% during the 1951-1980 period. In the Sahel, only ∼10% of the area was in severe wet or dry conditions in the 1960s, but it increased to ∼ 80% in the 1980s.

The long-term trends over the 1900-95 period are relatively small in the severe dry and wet areas (and the number frequency and severity of the severe dry and wet months). However, during the last 2-3 decades, there are some increases in the combined severe dry and wet areas, resulting from increases in either the dry area (e.g., over the Sahel, eastern Asia and southern Africa) or both the dry and wet areas (e.g., over the U.S. and Europe) (Fig. 2). Most of the increases occurred after 1970. Except for the Sahel, however, the magnitude of dry and wet areas of the recent decades is not unprecedented during this century.

An empirical orthogonal function (EOF) analysis of the PDSI revealed a leading mode (Fig. 3) that correlates significantly with ENSO events in time and space. This is not surprising in view of the well established changes in the distributions of rainfall, droughts and floods and throughout the world during the warm and cold phases of ENSO [e.g., *Kiladis and Diaz,* 1989; *Dai et al.,* 1997]. The temporal coefficients stay at a higher level after the late 1970s. The active regions of the EOF are the areas that exhibit the largest changes during the last 2-3 decades in the percentage areas (cf. Fig. 2), the number frequency, and severity of the severe dry and wet months, suggesting that this mode is primarily responsible for the recent changes in severe droughts and wet spells. The scatter plot (Fig. 4) of Fig. 3*a* reveals that the El Niño-induced PDSI anomalies are significantly higher during 1979-95 than would be expected using the 1900-78 relationship. The regression slope for 1900-78 is larger than that for 1979-95 when negative values of the SOI (as given by pressure at Darwin) are few. If the pre-1979 model is used to predict the PDSI coefficient, the upward shift around 1979 in the PDSI coefficient in Fig. 3a would largely disappear. *t*-tests on the difference of the means of the temporal coefficient before and after a given year yielded a peak *t*-value (∼29, significance level<0.01%) around 1978. This suggests that the ENSO-induced PDSI anomalies after about 1978 depart from what would be anticipated from the previous record. The ENSO EOF accounts for ∼7.8% of the global variance of the (normalized) PDSI. This number is considerably higher regionally over the U.S., the Sahel, southern Africa, Kazakhstan and southwestern Russia, northeastern China, and eastern Australia, and also higher if only ENSO years are considered. The ENSO EOF results primarily from the rainfall anomalies associated with ENSO

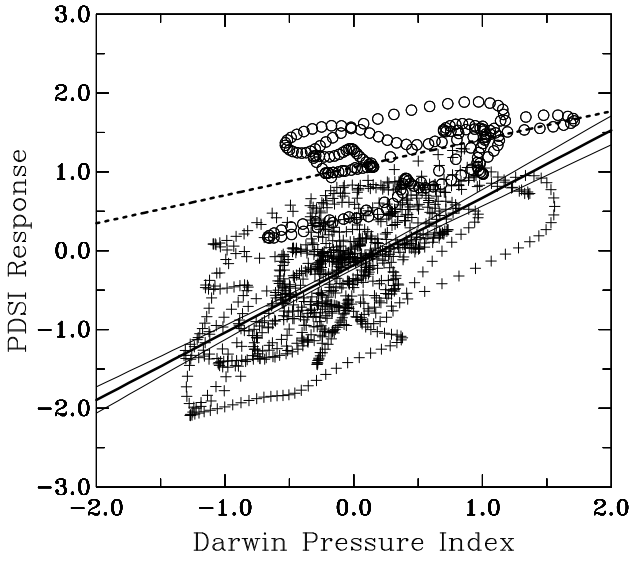

Figure 4. Scatter diagram of PDSI EOF1 coefficient (response) versus (6-month shifted) Darwin pressure index from Fig. 3*a*. The crosses are monthly data points for 1900-78 and the circles are for 1979-95. The thick solid line is the linear regression for 1900-78 and the thin lines are the 99% confidence interval for this regression line. The dashed line is the regression for 1979-95.

(Dai et al., 1997), while the contributions of temperature and possibly sampling errors are relatively small.

Discussion

Our PDSI results (Fig. 2) suggest that from 1900 to 1995 there are large multi-year to decadal variations in the percentage areas in severe drought and severe moisture surplus over many land areas while trends are small. During the last 2-3 decades there are some increases in the combined severe dry and wet areas over many ENSO-sensitive regions. In these regions, the ENSO-induced PDSI anomalies are larger during 1979-95 than would be expected based on the record of 1900-1978, consistent with the recent changes in the ENSO-rainfall relationship over Australia [*Nicholls et al.*, 1996b] and other regions [*Dai et al.*, 1997]. While it is still too early to distinguish the recent changes in the severe dry and wet spells from their multi-decadal variations seen over this century, there is a distinctive change in character evident. The shift of ENSO activity toward more warm phases after about 1976, which is very unusual given the record of previous 100 years [*Trenberth and Hoar*, 1996, 1997], has been linked to changes in evolution of ENSO [*Wang*, 1995] and decadal changes in climate throughout the Pacific basin [*Trenberth and Hurrell*, 1994; *Graham*, 1995]. Here we have further shown that the shift is also largely responsible for the recent changes in the PDSI over the ENSO-sensitive regions, and that there is an enhanced PDSI response for a given change in SOI. At the same time, global mean surface temperatures have increased rapidly since the late 1970s and the past 15 years are the warmest on record [*Nicholls et al.*, 1996a].

These coincidences raise the possibility that the global temperature increases, the ENSO changes and the jumps in ENSO-induced T, P and PDSI anomalies since the late 1970s could all result partly from the greenhouse gas-induced climate changes, which promote a more vigorous hydrological cycle. Moreover, some GCMs indicate a more El Niño-like climate (greater warming in the tropical east Pacific and an eastward shift of moist convection in the Pacific) superposed on top of more general warming with increased greenhouse gases [e.g., *Meehl and Washington,* 1996; *Knutson et al.,* 1995, 1997]. The model results need to be confirmed because GCMs still have deficiencies in simulating ENSO and the models themselves do not agree very well. However, the observational evidence strongly suggests that the global climate (specifically, T, P, the PDSI) have been changing toward an enhanced hydrological cycle response to ENSO in a way that is qualitatively consistent with expectations for anthropogenic climate change.

Acknowledgments. We thank T. Hoar for computer assistance and R. Madden and B. Bailey for their help on regression. A. Dai is supported by a NOAA Postdoctoral Program in Climate and Global Change fellowship, administered by the University Corporation for Atmospheric Research. NCAR is sponsored by the National Science Foundation.

References

Alley, W. M., The Palmer Drought Severity Index: limitations and assumptions. *J. Clim. Appl. Meteorol.* **23**, 1100-1109, 1984.

Barnes, R., UNESCO Flow Rates of Selected World Rivers, Monthly 1800-1972, *NCAR DS552.0*, NCAR Data Support Section, 1995.

Dai, A., I. Y. Fung, and A. D. Del Genio, Surface observed global land precipitation variations during 1900-1988. *J. Clim.* **10**, 2943-2962, 1997.

Graham, N. E., Simulation of recent global temperature trends. *Science* **267**, 666-671, 1995.

Gregory, J.M., J.F.B. Mitchell, and A. J. Brady, Summer drought in northern midlatitudes in a time-dependent CO_2 climate experiment. *J. Clim.* **10**, 662-686, 1997.

Hansen, J. and S. Lebedeff, Global trends of measured surface air temperature. *J. Geophys Res.* **92**, 13345-37, 1987.

Karl T. R. and R. W. Knight, Secular trends of precipitation amount, frequency, and intensity in the United States. *Bull. Am. Met. Soc.* **79**, 231-241, 1998.

Karl, T. R., et al., Indices of climate change for the United States. *Bull. Am. Met. Soc.* **77**, 279-292, 1995.

Kattenberg, A., et al., Climate models - projections of future climate. In: *Climate Change 1995: the Science of Climate Change*, Houghton, J.T., et al. (ed.), IPCC, Cambridge Univ. Press, Cambridge, pp.285-358, 1996.

Kiladis, G. N. and H. F. Diaz, Global climate anomalies associated with extremes in the Southern Oscillation. *J. Clim.* **2**, 1069-1090, 1989.

Knutson, T. R. and S. Manabe, Time-mean response over the tropical Pacific to increased CO_2 in a coupled ocean-atmosphere model. *J. Clim.* **8**, 2181-2199, 1995.

Knutson, T. R., S. Manabe, and D. Gu, Simulated ENSO in a global coupled ocean-atmosphere model: multidecadal amplitude modulation and CO_2 sensitivity. *J. Clim.* **10**, 138-161, 1997.

Meehl, G. A. and W. M. Washington, El Niño-like climate change in a model with increased CO_2 concentrations. *Nature* **382**, 56-60, 1996.

Nicholls, N., et al., Observed climate variability and change. In: *Climate Change 1995: the Science of Climate Change*, Houghton, J.T., et al. (ed.), IPCC, Cambridge Univ. Press, Cambridge, pp.133-192, 1996a.

Nicholls, N., et al., Recent apparent changes in relationships between the El Niño - Southern Oscillation and Australian rainfall and temperature. *Geophys. Res. Lett.* **23**, 3357-3360, 1996b.

Nicholson, S. E., An overview of African rainfall fluctuations of the last decade. *J. Clim.* **6** 1463-1466, 1993.

Palmer, W. C., Meteorological drought, *Res. Paper No.45,* 58pp., Dept. of Commerce, Washington,D.C., 1965.

Simpson, H.J., et al., Forecasting annual discharge of River Murray, Australia, from a geophysical model of ENSO. *J. Clim.* **6**, 386-390, 1993.

Slack, J.R., A. M. Lumb, and J. M. Landwehr, Hydro-Climatic Data Network (HCDN): streamflow data set, 1874 - 1988. *USGS Water-Resources Investigations Report* 93-4076, 1993.

Trenberth, K. E. and T. J. Hoar, The 1990-1995 El Niño - Southern Oscillation event: longest on record. *Geophys. Res. Lett.* **23**, 57-60, 1996.

Trenberth, K. E. and T. J. Hoar, El Niño and climate change. *Geophys. Res. Lett.* **24**, 3057-3060, 1997.

Trenberth, K. E. and J. W. Hurrell, Decadal atmosphere-ocean variations in the Pacific. *Clim. Dyn.* **9**, 303-319, 1994.

Vinnikov, K.Y. and A. Robock, Scales of temporal and spatial variability of midlatitude soil moisture. *J. Geophys. Res.* **101**, 7163-7174, 1996.

Wang, B., Interdecadal changes in El Niño onset in the last four decades. *J. Clim.* **8**, 267-285, 1995.

Webb, R. S., C. E. Rosenzweig, and E. R. Levine, Specifying land surface characteristics in general circulation models: soil profile data set and derived water-holding capacities. *Global Biogeochem. Cycles* **7**, 97-108, 1993.

A. Dai and K. E. Trenberth, National Center for Atmospheric Research, P.O. Box 3000, Boulder, CO 80307. (e-mail: adai@ucar.edu; trenbert@ucar.edu)

T. R. Karl, NOAA National Climatic Data Center, Asheville, NC 28801. (e-mail: tkarl@ncdc.noaa.gov)

(Received March 10, 1998; revised July 22, 1998;
accepted July 27, 1998.)